Astron. Astrophys. 189, 353–360 (1988)

ASTRONOMY AND ASTROPHYSICS

First results with a transmission echelle grating on the ESO Faint Object Spectrograph: observations of the SN 1986a in NGC 3367 and of the nucleus of the galaxy

H. Dekker, S. D'Odorico*, and R. Arsenault

European Southern Observatory, D-8046 Garching bei München, Federal Republic of Germany

Received April 13, accepted July 6, 1987

Summary. The characteristics of a 79 lines/mm transmission echelle grating mounted on the ESO Faint Object Spectrograph and Camera (EFOSC) are presented. In combination with a cross disperser grism, this new grating gives on a single CCD frame spectra at a resolving power of about 2000. Two different cross-dispersers are used to select the $\lambda\lambda$4000–7500 Å and $\lambda\lambda$5500–9500 Å regions respectively. The peak efficiency of the echelle is 44%. The measured global efficiency of the 3.6 m telescope + instrument (echelle mode) + detector is such that 1 photon s^{-1} $Å^{-1}$ is detected from a star of $m_v = 17$.

Observations of the type I SN 1986a in the spiral galaxy NGC 3367 and of the Seyfert-like nucleus of the same galaxy were obtained during the tests of the echelle grating. The B and V magnitudes of the SN and of the stellar nucleus of the galaxy were measured from CCD frames of the galaxy. For the supernova and the nucleus, $m_v = 14.55$ and 14.50 respectively on Feb. 19.1, 1986, U.T. The SN shows a type I spectrum. Two narrow and faint (EW $\simeq$ 300 mÅ) absorption features in the spectrum of the SN are attributed to Na I interstellar gas in the disc of the galaxy, indicating that the SN is either within the disc or on the far side of it with respect to the observer.

The spectrum of the nucleus shows strong emission lines in the Balmer series of hydrogen, and the forbidden lines of [O III] and [N II]. The profiles are broad and asymmetrically extended toward the blue.

Key words: instruments – supernovae – Seyfert galaxies

1. Introduction

EFOSC, the European Southern Observatory (ESO) Faint Object Spectrograph and Camera, is a focal reducer with spectroscopic capability which uses a RCA CCD as a detector. It has been in operation since March 1985 at the F/8 Cassegrain Focus of the ESO 3.6 m telescope on La Silla. With the F/2.5 camera of EFOSC, one pixel (30 μm) corresponds to 0.″675. The pupil has a diameter of 40 mm. In the parallel beam of the instrument filters or transmission grisms can be inserted, mounted on two separate 12-position wheels. A third wheel is located in the focal plane of the telescope, again with 12 positions where slits of different width and length or specially prepared aperture plates can be mounted. A description of the instrument and of its modes of operation can be found in Dekker and D'Odorico (1985, 1986) and D'Odorico and Dekker (1986). EFOSC is characterized by high efficiency and versatility. The observer has the choice between six remotely interchangeable modes of observation: direct imaging, slitless grism spectroscopy, long slit spectroscopy, multiple object spectroscopy, field polarimetry and echelle spectroscopy. In the first part of this paper we report in detail about this latter mode and in particular about the properties of the transmission echelle grating. In the second part, the observations of the SN 1986a in NGC 3367 and of the nucleus of the same galaxy obtained with the echelle grating are presented to illustrate the instrumental capabilities. Their astrophysical significance is also briefly discussed.

Send offprint requests to: S. D'Odorico

* On leave from Dipartimento di Fisica, Università di Calabria, Italy

2. The transmission echelle grating in EFOSC

The interest in a transmission echelle arose from the wish to increase the highest spectral resolution which can be obtained with EFOSC (7 Å with a 1.″5 wide slit). One can easily show that the linear dispersion given by a grism is

$$\frac{\delta\lambda}{\delta x} = \frac{\lambda}{W.F\#.(n-1)\,\mathrm{tg}\,i}, \qquad (1)$$

where W is the width of the grating, $F\#$ the speed of the camera, n the index of the resin and of the substrate (taken to be the same) and i the angle of the prism. W, $F\#$ and n are fixed because of instrument construction constraints, pixel matching considerations and availability of resins, respectively. Equation (1) clearly shows the well-known rule that the dispersion in a grating spectrograph depends on the angle of incidence on the grating once the optical parameters of the spectrograph are fixed. The maximum dispersion that can be reached with the normal grisms in EFOSC is 120 Å/mm, corresponding to $i = 40°$ ($\mathrm{tg}\,i = 0.8$). Grisms with a larger prism angle and higher groove frequency, to provide higher dispersion in first order, are not feasible. A transmission echelle with $\mathrm{tg}\,i = 2$ ($i = 63°.4$) would increase the dispersion by a factor of 2.5 to about 50 Å/mm. Standard EFOSC grisms can easily provide the cross-dispersion to separate properly the spectral orders. In one CCD frame one can obtain a coverage of 3000 Å, split into 6–9 orders, a format that is definitely of interest for many observing programs.

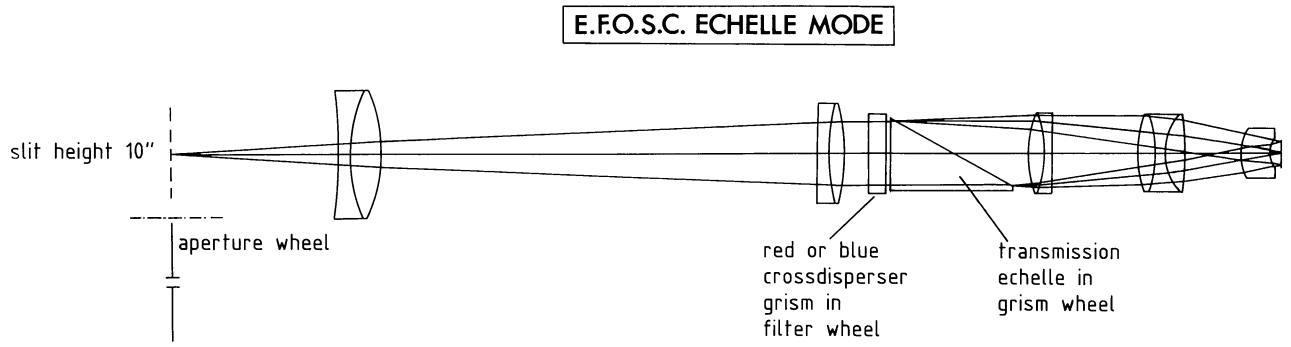

Fig. 1. Optical layout of EFOSC in the echelle mode. The cross-dispersing grism is mounted in the filter wheel, the transmission echelle in the grism wheel

Table 1. Characteristics of the EFOSC transmission echelle and cross dispersers

Echelle	
Glass substrate	BK7
Blaze wavelength	589 nm in 10th order
Groove frequency	79 lines/mm
Groove angle	63°.4
Blue Cross Disperser (BCD)	
Glass substrate	BK7
Blaze wavelength	450 nm
Groove frequency	200 lines/mm
Groove angle	10°
Red Cross Disperser (RCD)	
Glass substrate	BK7
Blaze wavelength	700 nm
Groove frequency	100 lines/mm
Groove angle	7°.6

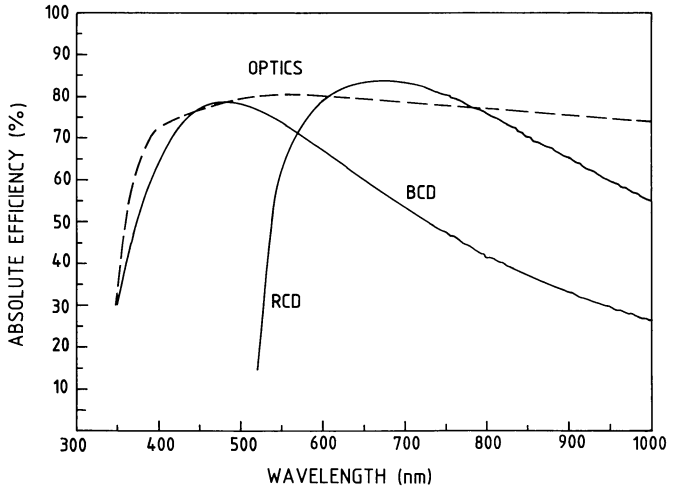

Fig. 2. Efficiency of the 200 lines/mm blue cross-dispersing grism, the 100 lines/mm red cross-dispersing grism (BCD and RCD, respectively) and of the EFOSC optics

It should be pointed out that transmission echelles provide less resolution and dispersion than their reflection equivalents. The linear dispersion of a reflection echelle is

$$\frac{\delta\lambda}{\delta x} = \frac{2\lambda}{W.F\#.\,\mathrm{tg}\,i}, \qquad (2)$$

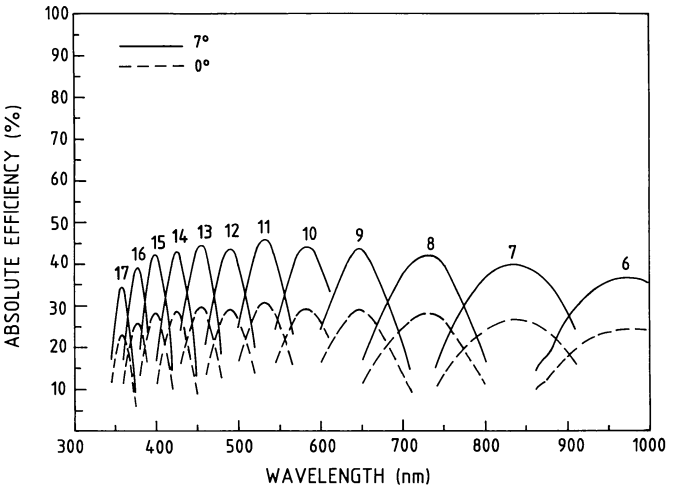

Fig. 3. Efficiency in orders 6–17 of the 79 lines/mm transmission echelle at 0° (lower curves) and 7° (upper curves) inclination angle of the echelle grism. The echelle is presently mounted on EFOSC at an angle of 7°

and so the dispersion of a reflection echelle is greater by factor of $2/(n-1)$; about 3.5 for practical values of n. It is clear that a transmission echelle only makes sense if it is used to extend the possibilities of a low-dispersion (grism) spectrograph.

Bausch and Lomb have built a transmission echelle for a U.S. customer. The results were satisfactory and the concept of a high angle transmission system seems to be validated. Even though we could not find any reference to astronomical observations obtained with that grating, we considered the matter sufficiently encouraging to test an echelle on EFOSC. Parameters of the echelle ifself and of two cross-dispersers (one for the blue-visual region and one for the red) were computed by one of us (H.D.), using a first-order theory. Table 1 lists the characteristics of these three gratings. The prismatic BK7 substrates were manufactured by a local manufacturer, while Bausch and Lomb replicated the gratings. The entrance face of the echelle prism is coated with a single layer of MgF_2, peaked at 550 nm. Figure 1 shows the optical layout of EFOSC with the echelle and cross-disperser inserted in the beam. Figures 2 through 4 show the optical efficiencies of the various components of the optical system. Cross-dispersers have an efficiency similar to that measured for the other EFOSC grims and reported in Dekker and D'Odorico (1985).

The average efficiency of the echelle grating turned out to be lower than expected, about 30% at the peak of the blaze function. After conducting a series of tests, an improvement of about a

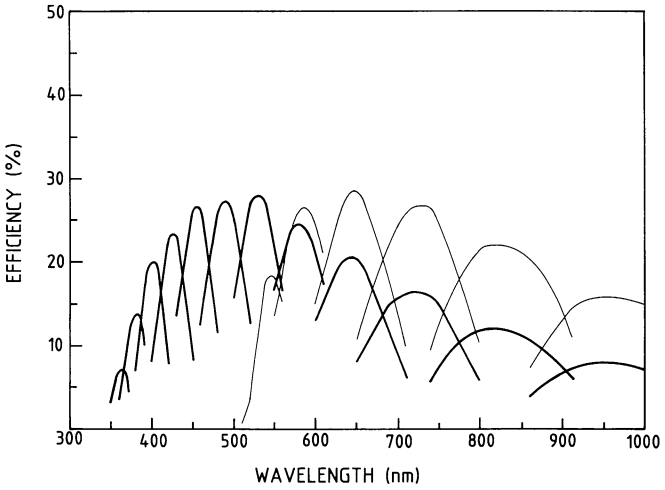

Fig. 4. The overall optical efficiency of EFOSC in echelle mode, obtained by multiplying the efficiencies of optics, echelle and BCD (thick curves) or RCD (thin curves)

Table 2. Wavelength coverage and pixel size of EFOSC in echelle mode

	Order number	Wavelength coverage (Å)	Pixel size (Å)
BCD [a]	15	3780–4280	1.0
	14	4020–4560	1.1
	13	4300–4900	1.2
	12	4630–5280	1.3
	11	5010–5730	1.4
	10	5480–6280	1.6
	9	6050–6940	1.7
	8	6780–7800 [b]	1.9
RCD [a]	7	7710–8890	2.2
	6	8960–9800 [c]	2.5

[a] BCD: with the Blue Cross Disperser
RCD: with the Red Cross Disperser
[b] With the BCD limited to 7500 Å by the CCD size
[c] Limited by CCD quantum efficiency and second order overlapping

factor 1.5 was realized by mounting the echelle at an inclination of 7° from its normal angle. It is this latter efficiency which is plotted in Fig. 4. The reduced efficiency at 0° mounting angle is probably due to the groove shape. ESO is now conducting a series of tests on the 79 lines/mm and other echelle gratings in collaboration with Bausch and Lomb, in an attempt to further improve the efficiency. The intensity of stray light in the echelle spectrum obtained with EFOSC is remarkably low or less than 1% in the interorder space.

3. The format, resolution and efficiency of the EFOSC echelle mode

The data which are reported here refer to an observing run in February 1986 with the transmission echelle no. 1 mounted with zero inclination on EFOSC at the 3.6 m telescope. The grating no. 2 is the one that is available for general use as of October 1986, and gives a slightly lower dispersion due to the 7° inclination at which it is used. The maximum slit length which is permitted without order overlapping is 10″ for both cross-dispersers. ESO CCD #3 was used as a detector. It is an RCA SID 501 thinned, backside illuminated device, with 512 × 320, 30 μ^2 pixels. It has a peak quantum efficiency of more than 80% at 5500 Å and a read out noise of 40 e^-. Table 2 gives the wavelength coverage and the pixel size for each order in the two options.

The transmission echelle is mounted in one of the grism positions on the EFOSC grism wheel. Both cross-disperser grisms are mounted in front of the echelle, in the filter wheel. Other grisms, filters, etc. can also be mounted at the same time. Changing from echelle mode to another mode is accomplished in a matter of seconds since all functions are remotely controlled.

These data have been obtained by reducing the spectra with a modified version of the echelle reduction program available in the MIDAS (Munich Image Data Analysis System) data reduction package. For the red cross-disperser spectra, neon and argon lamps can be used with good results for wavelength calibration. For the blue cross disperser, the observer must combine the spectra of the argon, cesium and helium lamps to get a sufficient number of lines in all orders. The r.m.s. error of the polynomial fitting to the calibration lines is 0.25 Å or 12.5 km s^{-1} at $\lambda = 6000$ Å.

Most of the spectra in the February 1986 run were obtained with a 1 arcsec wide slit, which projects on 1.5 pixels of the detector. The actual resolution was estimated from the FWHM of comparison lamp and sky lines in the reduced spectra. These measurements were quite consistent and indicate FWHMs of 2.6 Å at 5500 Å in order No. 12 (resolving power $\lambda/\Delta\lambda = 2100$) with values in the other orders changing according to the pixel size in Å.

The efficiency of EFOSC in the echelle mode can be derived from the well measured efficiency of the standard grism mode (1 photon s^{-1} Å^{-1} for a star of $m_v = 18.2$ at 5500 Å). With an average efficiency of the echelle grating of 0.40 (Fig. 4) the global value for this mode corresponds to 1 photon s^{-1} Å^{-1} for a star of about 17th magnitude. This value is confirmed by observations of standard stars with a wide slit. It implies that S/N ratios of at least 30 can be obtained for an object of $m_v = 18$ in a 90 minute exposure.

4. Photometry and echelle spectroscopy of the SN 1986a and of the nucleus of NGC 3367

4.1. The observations

The discovery of a supernova in the barred SBc galaxy NGC 3367 was reported by Evans (1986) and then confirmed by the independent finding of Leibundgut and Cameron (1986). Observations of the SN 1986a using EFOSC in the echelle mode provided a unique opportunity to search for interstellar features in its spectrum. The SN in NGC 3367 ($m_B \simeq 15.$) was too faint to be studied with the ESO Echelle spectrograph CASPEC as has been done for the SN 1983n in M83 (D'Odorico et al., 1985), SN 1984j in NGC 1559 (D'Odorico and Bergeron, 1987) and SN 1986g in NGC 5128 (D'Odorico et al., 1987).

Table 3. Journal of the observations

Object	Observing mode [a]	Filter/grating	Exposure time (s)	Date (U.T.)
NGC3367	I	6562/150	900	Feb. 19.00
Nucleus NGC3367	S	Echelle+BCD	1800	Feb. 19.02
SN1986a	S	Echelle+BCD	1800	Feb. 19.06
NGC3367	I	*V*	20, 35	Feb. 19.09
NGC3367	I	*B*	20	Feb. 19.09
NGC3367	I	6634/70	900	Feb. 20.05
NGC3367	I	6562/60	900	Feb. 20.06

[a] Observing modes – *I*: imaging; *S*: spectroscopy with the echelle grating

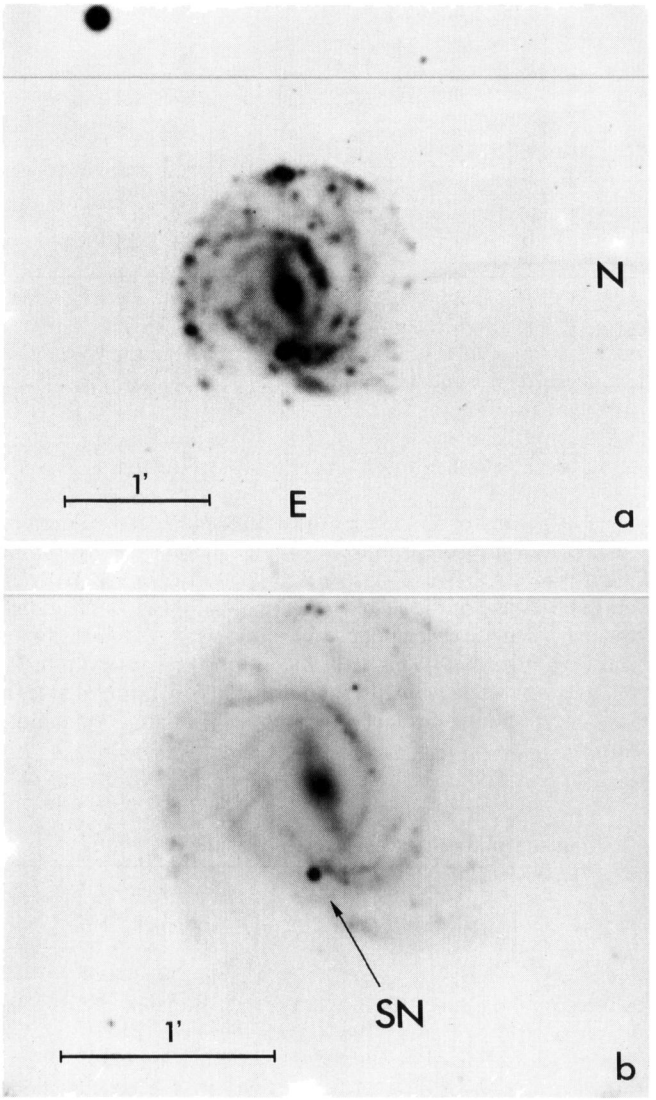

Fig. 5a and b. Two CCD images of NGC 3367 obtained with EFOSC **a** through an interferential filter (70 Å FWHM) centered on λ6654 Å (Hα). **b** In the *V* colour

The nucleus of NGC 3367 was known to have strong and relatively broad emission lines. The systemic radial velocity of 3034 km s^{-1} (Sandage and Tammann, 1981, hereafter referred to as SAC) places it at 58 Mpc using $H_0 = 50$ km s^{-1} Mpc^{-1}. The galaxy is seen almost face-on (axial ratio = 0.91).

Véron-Cetty and Véron (1986) have included the nucleus in their spectroscopic survey of galaxy nuclei. They classify it as a N galaxy (that is nucleus of stellar appearance with Seyfert-like spectrum, i.e. Hα < 1.2 [N II] 6584 Å) but pointed out some peculiarities in the line intensities. We have obtained an echelle spectrum of the nucleus to study the line profiles at higher resolution.

The observations of NGC 3367 and its supernova provide a good example of the multimode capability of EFOSC. Beside the echelle spectra of the SN and of the nucleus, we have obtained direct images of the galaxy in *B* and *V* colours and through narrow filters (FWHM = 60 Å) centered at the wavelength of Hα at the redshift of the galaxy and in the nearby continuum (6634 Å and 6562 Å respectively). Table 3 presents the log book of the observations.

Figures 5a, b show two of the direct images of the galaxy. The Hα picture outlines a disturbed spiral structure with many bright H II regions. The SN is projected close to one of the brightest H II regions, but the exposure in the visible obtained in better seeing conditions shows clearly that it falls in the interarm region.

The magnitudes of the supernova and of the bright, stellar nucleus of the galaxy were derived from the observations of 6 standard stars in the field E2 and NGC 3201 observed by Graham (1982) and Alcaino and Liller (1984) respectively. The SN 1986a *B* and *V* magnitudes measured on February 19.09 UT are as follows: $B = 15.05\,(+0.05)$ and $V = 14.55\,(+0.05)$. The NGC 3367 nuclear magnitudes are: $B = 15.5$ and $V = 14.5$. No correction for the absorption was applied. These magnitudes would indicate that the supernova has become 0.55 magnitudes fainter compared to the measurement made by Evans on Feb. 4th. This corresponds to a light fall in *B* of 0.07 mag/day. The $(B-V)$ colour of 1986a is about 0. near maximum (IAU Circulars 4173 and 4175), and 0.5, 15 days later (our photometry). Type I SN's usually have a $(B-V)$ colour of 0.0 near maximum light, increasing monotonically to a value of $(B-V) \sim 1.0$ about one month later (Barbon et al., 1982). Furthermore, during the first month after maximum, the blue light of such SN's decreases at a rate of 0.075 mag/day. These values are in very good agreement with the observed characteristics of 1986a, except for the *B* magnitude of 13.7 reported by Barbon and Ciatti in IAU Circular 4177. This *B* magnitude is

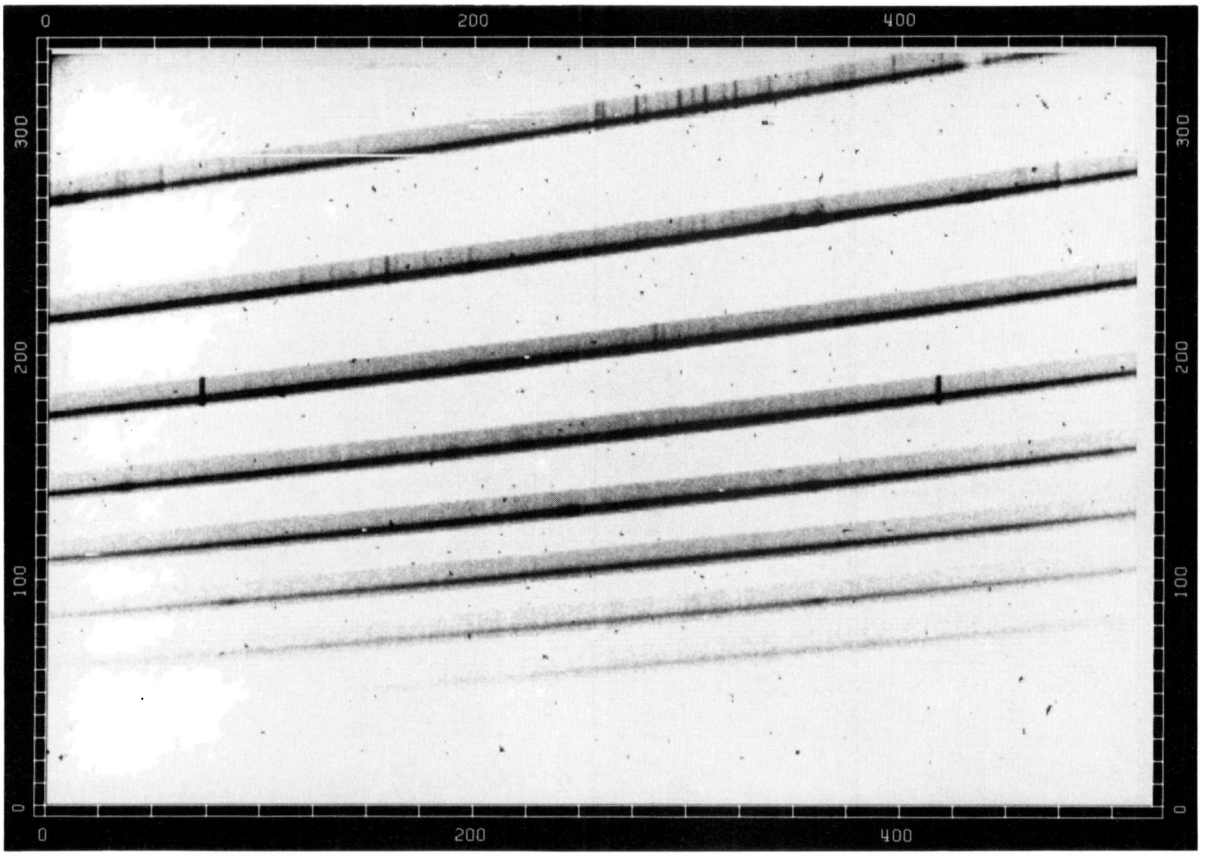

Fig. 6. The echelle spectrum of the stellar nucleus of NGC 3367 obtained with EFOSC. The resolving power is about 2000. The visual magnitude of the nucleus is 14.50, the exposure time was 30 minutes. Hα with the [N II] satellites and the [S II] doublet are seen in the second order from the top, Hβ and [O III] in the fifth. The sky line [O I] λ5577 Å is seen in the two central orders

inconsistent with the other data. Ignoring this value for the time being, the behaviour of 1986a appears absolutely normal, that is the colour and light fall are consistent with the average behaviour of type I SN's.

4.2. *The echelle spectrum of the nucleus of* NGC 3367

Figure 7 shows a spectrum of the nucleus of NGC 3367. One can identify the emission lines Hγ, Hβ, [O III] 4959;5007 Å, Fe II 5198 Å, He I 5876 Å, [O I] 6300 Å, Hα, [N II] 6548;6584 Å, and [S II] 6716;6730 Å.

The following line ratios have been measured in our spectrum and are in very good agreement with the values derived by Véron-Cetty and Véron (1986): Hα/[N II] 6584 = 1.12; Hβ/[O III] 5007 = 2.2 and [O I] 6300 Å amount to 5% of Hα. The [S II] density densitive doublet gives a ratio 6717/6730 = 0.77 which corresponds to $N_e \sim 3000\,\mathrm{cm}^{-3}$ if the kinetic temperature is assumed to be 10 000 K (Osterbrock, 1974). This value of density is typical for narrow line regions of Seyfert 2 galaxies (Whittle, 1985). As noted by Véron-Cetty and Véron (1986) the line intensity ratios are difficult to interpret. They are clearly different from those of an H II region ionized by hot stars, but they also differ from a Seyfert 2 spectrum ([O III]/Hβ too small) or that of a LINER ([O I]/Hα too small). Both the hydrogen and forbidden lines are broader than the instrumental profile. A careful examination of the line profiles, especially in the blue part of the spectrum, shows clearly a blue asymmetry (see Fig. 8). This is consistent with the finding of Véron-Cetty and Véron (1986), who obtained the best fit to the Hα and [N II] 6548 and 6584 blend with two sets of 3 lines (see their Fig. 1). Blue asymmetries are a common feature in the emission lines of Seyferts and AGN's. They have been interpreted as ejection of matter from an active nucleus. The blueshifted ejection is better seen since it is less obscured by the homogeneous dust distribution. In another scenario, it has been suggested that they are due to infall of matter on the active nucleus. Combination of conditions such as small covering factor of the ionizing source and internal dust in the emitting clouds favours the observation of the gas on the opposite side of the nucleus (Whittle, 1985). In order to investigate the line profiles in more detail, we have carried out a multi-gaussian fit to the emission lines. The multicomponent analysis of the Hβ and [O III] 5007 Å lines is easier than for the Hα and [N II] blend or for the [S II] doublet since Hβ and [O III] 5007 Å are clearly separated. It was realized that when the blueshift of the Hβ secondary component (SC) was not constrained to be the same as the [O III] 5007 Å SC, a much better fit was obtained. The results are that the FWHM of the [O III] 5007 Å main component (MC) is 8.1 Å, while the Hβ MC has a FWHM of 3 Å (both corrected for instrumental broadening). The [O III] SC is more blueshifted ($-530\,\mathrm{km\,s}^{-1}$) with respect to the MC than the Hβ SC ($-150\,\mathrm{km\,s}^{-1}$). The FWHM's of the SC's are 11.5 and 7.0 Å for Hβ and [O III] 5007 Å respectively. The former value is highly uncertain since the Hβ components are less separated and the FWHM of the SC is very sensitive to he parameters adopted for

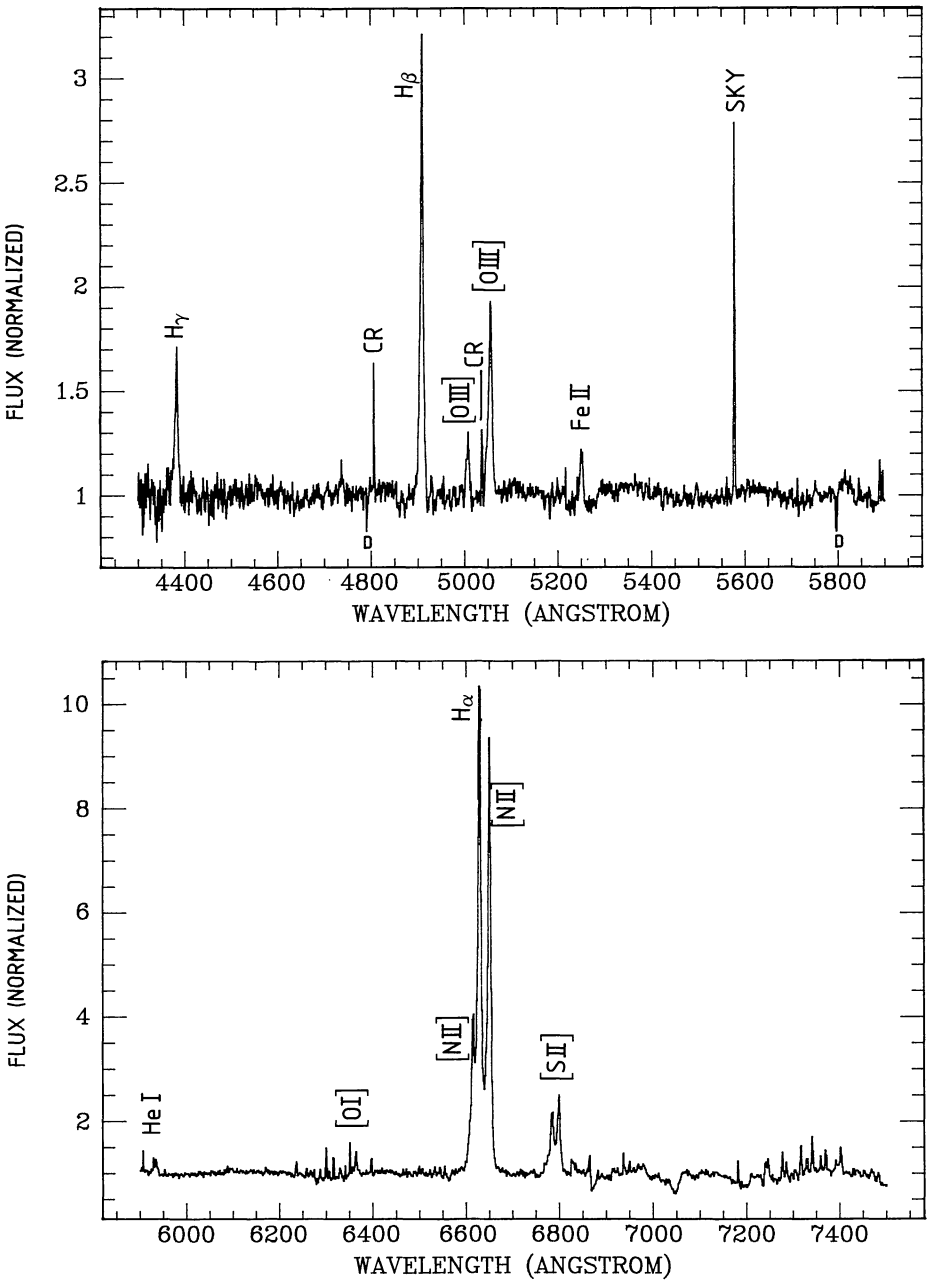

Fig. 7 a and b. Two extracted and wavelength calibrated orders of the echelle spectrum of the nucleus of NGC 3367. Radiation events (CR) and low efficiency pixels of the CCD (D) are identified. **a** Hβ and [O III] region. Average resolution is 2.6 Å. **b** Hα, [N II] and [S II] emission line region. Average resolution is 3.2 Å

the MC in the fitting and the signal to noise ratio in the wings of the line. The fit shown in Fig. 8 is based on the above parameters.

In a second step, we have examined the radial velocities given by the main components of the emission lines. We found that the radial velocity measured with the [O III] 5007 Å line is significantly smaller than the one measured with the other lines. The radial velocity given by the [O III] 5007 Å line is 2950 km s^{-1}, while the mean radial velocity given by all other lines is 3018 ± 6 km s^{-9}.

4.3. The spectrum of the SN 1986a in NGC 3367

Most of the spectral features reported in the IAU circulars on SN 1986a (in particular circular 4201) can clearly be seen in our spectrum (Fig. 9). The most prominent are the absorption bands of Fe II 4568 Å, 4924 Å, 5215 Å, and 5535 Å, blueshifted by a considerable amount. It is also possible to see the strong absorption feature attributed to Si II 6355 Å. This last feature is characteristic of type I SN's. The P Cygni profile can be recognized in the strong emission features, especially at ~4600 Å (Fe II 4568 Å).

The series of spectra taken by Branch et al. (1983) of the type I SN 1981b in NGC 4536 provide good camparison data. They illustrate the spectral evolution of the SN spectrum from maximum light up to 100 days later. Following their interpretation, we consider the very large absorption and emission features in the spectrum of SN 1986a, as P Cygni profiles of the lines identified before. We have measured the absorption feature centroids, in order to get the expansion velocity of the material ejected by the

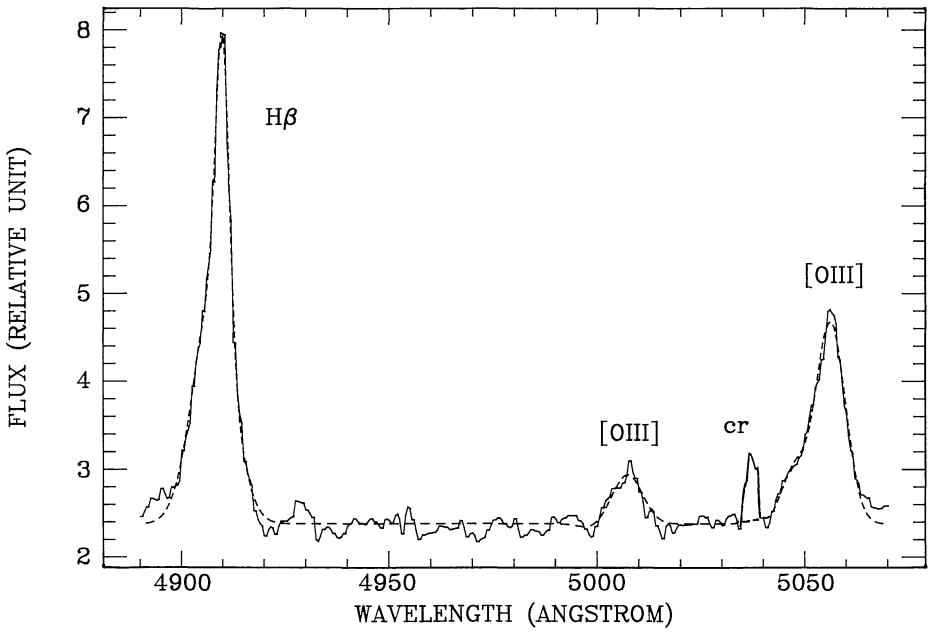

Fig. 8. An expanded view of the Hβ-[O III] spectral region of the spectrum of the nucleus of NGC 3367. The broad asymmetrical structure of the emission lines is well visible at this scale. The broken line shows the fit to the profiles with the two gaussian components. FWHM's of the main components are 3 Å for Hβ and 8 Å for [O III]

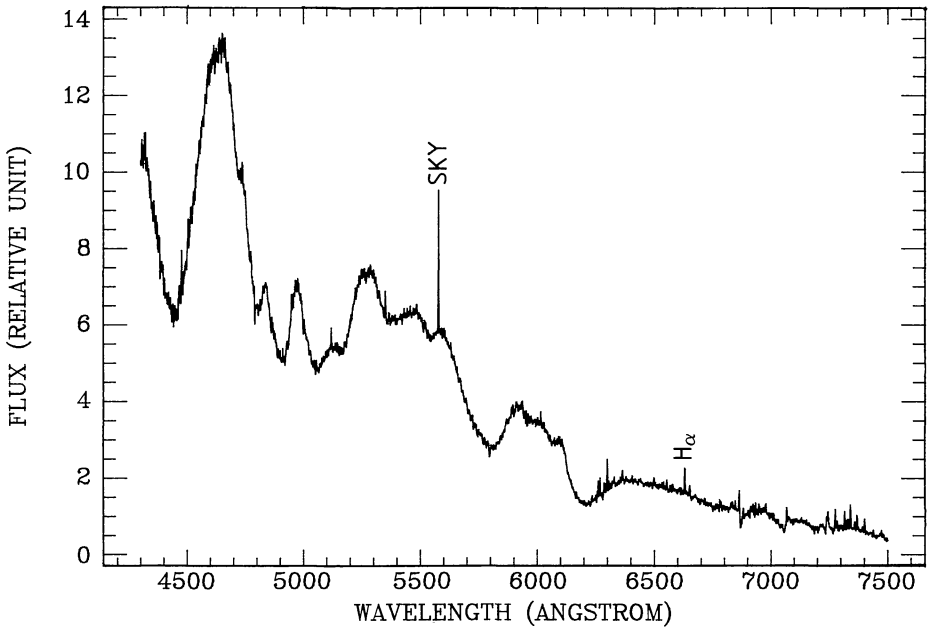

Fig. 9. The extracted and merged spectrum of the SN 1986A in NGC 3367 from the echelle grating exposure with EFOSC. An observation of a standard star was used to correct for the blaze function. The narrow emission is identified as Hα from the ionized gas in the disc of the galaxy (NGC 3367), falling within the observing aperture but not associated with the SN

supernova. The mean value of the expansion velocity is 10150 km s^{-1}, in very good agreement with other observations of supernovae shortly after maximum light (Sadler and Richtler, 1983; Branch et al., 1983). The different expansion velocity measured from the 5892 Å Na I feature (7500 km s^{-1}) is predicted by models and indicates a velocity and abundance structure of the expanding shell, detected by observing lines of different optical depth.

4.4. Interstellar absorption features in the line of sight to NGC 3367

As mentioned above, the SN in NGC 3367 provided the opportunity to detect absorbing clouds in the line of sight to NGC 3367. The spectra were systematically explored for the Ca II and Na I absorption lines and for diffuse interstellar bands at velocities between 0 and 3100 km s^{-1}.

The Na I doublet is clearly detected in the spectrum of the SN 1986a, with equivalent widths of 280 mÅ and 334 mÅ for the 5890 Å and 5896 Å lines respectively. The detection limit in the Na I region is 170 mÅ. The doublet gives a redshift of 3084 km s^{-1}, which corresponds fairly well to the systemic velocity of NGC 3367 (SAC). Indeed, a weak narrow Hα emission, seen in the SN spectrum, gives a radial velocity of 3094 km s^{-1}, in very good agreement with the Na I doublet value. Since the Hα emission is likely to come from the nearby H II region seen in the disk of NGC 3367 close to the projected position of the SN, the velocity agreement confirms that the Na I absorbing gas is associated with the disk and that the SN is either embedded in the disk or behind it.

In the Ca II H and K lines region the limit of the detection is 220 mÅ. There is an absorption feature which could correspond to Ca II H redshifted to the proper wavelength, but it is marginally detected (less than 3σ) and has no obvious K counterpart.

The Ca II H and K and the Na I doublets in the rest frame of NGC 3367 are not detected in the spectrum of the nucleus. Using the formula derived by Hobbs (1984), one can put an upper limit of 500 mÅ and 200 mÅ on the equivalent width of Ca II H and K and Na I 5890, 5896 Å respectively. The lower upper limit of the Na I doublet comes from the fact that the signal to noise ratio is higher in this wavelength range.

No absorption lines were detected at galactic ($V \sim 0\,\mathrm{km\,s^{-1}}$) or intermediate velocities. This is consistent with the galactic coordinates of NGC 3367 ($l = 231°$, $b = 58°$) and the detection limits quoted above.

5. Conclusions

A new configuration of EFOSC has been presented, which uses an echelle grating and a cross-disperser to provide moderate-high resolution spectra (resolving power ~ 2000) of astronomical objects. In the ESO Faint Object Spectrograph one can now change in a matter of seconds from an imaging mode to long slit grism or echelle spectroscopy. Moreover, this versatility is allied to a high efficiency. For the echelle configuration a $m_v = 17$ star gives an output of 1 photon $\mathrm{s^{-1}\,Å^{-1}}$ at the 3.6 m telescope.

Observations of the SN 1986a in the galaxy NGC 3367 and of the galaxy nucleus have been presented in order to illustrate the possibilities of the echelle mode. The B and V magnitudes of the SN are in good agreement with results from other type I supernovae, from the point of view of light fall and colour. The spectrum of SN 1986a exhibits the wide emission and absorption bands usually attributed to the P Cygni profiles of Fe II, Si II, and Na I lines. The mean expansion velocity of the ejected material is $10\,500\,\mathrm{km\,s^{-1}}$ as measured from the absorption dips in the SN spectrum.

The bright, stellar nucleus of NGC 3367 shows the usual emission lines observed in Seyfert galaxies, though the line ratios are puzzling. The brightest emission lines have been used to carry out a multi-component analysis with gaussian profiles. The lines present a blue asymmetry which is best seen in Hβ and [O III] 5007 Å. They could be fitted with two gaussians with a variable separation. The main components of these fits are relatively broad with FWHM of ~ 3 Å for Hβ and 8 Å for [O III] 5007 Å. The redshift measured with the [O III] 5007 Å line is significantly smaller than the one given by the other lines.

The Na I 5890 and 5896 Å absorption lines are detected in the SN spectrum in the reference frame of NGC 3367, with an EW of 280 and 330 mÅ, showing that the SN is either in the disk of NGC 3367 or behind it.

Acknowledgements. We would like to thank M. Véron-Cetty for communicating the results on the spectra of the nucleus of NGC 3367 in advance of publication. B. Buzzoni has carried out the systematic investigation on the efficiency of the transmission echelle. D. Ponz has updated the echelle reduction package in MIDAS to allow for a semi-automatic reduction of the EFOSC echelle data. One of us (R.A.) acknowledges the National Sciences and Engineering Research Council of Canada for a postdoctoral fellowship and the European Southern Observatory for its support and hospitality.

References

Alcaino, G., Liller, W.: 1984, *Astron. J.* **89**, 1713
Barbon, R., Ciatti, F., Rosino, L., Ortolani, S., Rafanelli, P.: 1982, *Astron. Astrophys.* **116**, 43
Barbon, R.: 1986, IAU Circ. **4177**
Binette, L.: 1985, *Astron. Astrophys.* **143**, 334
Branch, D., Lacy, C.H., McCall, M.L., Sutherland, P.G., Uomoto, A., Wheeler, J.C., Wills, B.J.: 1983, *Astrophys. J.* **270**, 123
Dekker, H., D'Odorico, S.: 1985, ESO Operating Manual No. 4
Dekker, H., D'Odorico, S.: 1986, *The Messenger* **46**, 21
D'Odorico, S., Pettini, M., Ponz, D.: 1985, *Astrophys. J.* **299**, 852
D'Odorico, S., Dekker, H.: 1986, Proceedings of the Workshop on the Optimization of the use of the CCD detectors in Astronomy, eds. J. Baluteau, S. D'Odorico, p. 315
D'Odorico, S., Bergeron, J.: 1987 (in preparation)
D'Odorico, S., di Serego Alighieri, S., Magain, P., Nissen, P., Panagia, N.: 1987 *Astron. Astrophys.* (submitted)
Evans, R.D.: 1986, IAU Circ. 4173
Graham, J.A.: 1982, *Publ. Astron. Soc. Pacific* **94**, 244
Hobbs, L.M.: 1984, *Astrophys. J.* **280**, 132
Leibundgut, B., Cameron, L.: 1986, IAU Circ. 4175
Osterbrock, J.E.: 1974, in *Astrophysics of Gaseous Nebulae*, Freeman, San Francisco, p. 112
Pearce, G., Ellis, R., Parry, I., Reid, I.N.: 1986, IAU Circ. 4201
Richtler, T., Sadler, E.M.: 1983, *Astron. Astrophys.* **128**, L3
Sandage, A., Tammann, G.A.: 1981, "A Revised Shapley-Ames Catalog of Bright Galaxies" (Washington: Carnegie Institution of Washington) (SAC)
Véron-Cetty, M.P., Véron, P.: 1986, *Astron. Astrophys. Suppl. Ser.* **66**, 335
Whittle, M.: 1985, *Monthly Notices Roy. Astron. Soc.* **213**, 1